We are IntechOpen, the world's leading publisher of Open Access books Built by scientists, for scientists

4,800
Open access books available

122,000
International authors and editors

135M
Downloads

Our authors are among the

154
Countries delivered to

TOP 1%
most cited scientists

12.2%
Contributors from top 500 universities

CLARIVATE ANALYTICS BOOK CITATION INDEX INDEXED

WEB OF SCIENCE™

Selection of our books indexed in the Book Citation Index in Web of Science™ Core Collection (BKCI)

Interested in publishing with us?
Contact book.department@intechopen.com

Numbers displayed above are based on latest data collected.
For more information visit www.intechopen.com

Chapter 3

Photonic Crystal Chemical/Biochemical Sensors

Saeed Olyaee, Hamideh Mohsenirad and
Ahmad Mohebzadeh-Bahabady

Additional information is available at the end of the chapter

http://dx.doi.org/ 10.5772/63288

Abstract

In this chapter, the definitions of the photonic crystals (PhCs) are presented and the photonic crystal-based sensors are described. The structures of some photonic crystal biosensors that can detect chemical or biochemical molecules are also investigated. Sensing mechanism in the most photonic crystal sensors is based on the refractive index (RI) change mechanism. By binding the chemical or biochemical molecules to active sensing surface, the refractive index will be changed. So, the resonant wavelength or the intensity of the transmission spectrum is changed. This process can be used as a way to measure the concentration of the molecules. To simulate the optical wave behavior in the structure and evaluating the ability of biosensing, the two-dimensional finite-difference time-domain (2D-FDTD) and plane-wave expansion (PWE) methods are used. The sensors that are presented in this chapter are mostly based on photonic crystal resonators. Some structures based on micro-/nano-resonators, structures based on LX resonators, and structures based on ring resonator are investigated. Important parameters on sensing applications for these structures are also calculated.

This chapter is organized as follows: an introduction to photonic crystal structures is presented in Section 1. Then, sensing mechanism in chemical sensors based on photonic crystals is described in Section 2. Quality factor, full width at half maximum (FWHM), free spectral range (FSR), detection limit (DL), and sensitivity are the most important parameters in sensing applications which are introduced in Section 3. Finally, the last section describes some structures of photonic crystal chemical/biochemical sensors.

Keywords: photonic crystal, nanostructures, chemical sensor, biochemical sensor, micro-/nano-resonator

1. Introduction

In recent years, designs of optical devices based on periodic structures have been widely developed. One of the periodic structures that can control and guide the photons is photonic crystal (PhC). Photonic crystals are the periodic dielectric structures that can be categorized into three main groups as one-dimensional (1D), two-dimensional (2D), and three-dimensional (3D) structures [1].

A good example of 1D PhCs is the Bragg grating which the periodic dielectrics of structures occur in one direction, while in two other directions structure is uniform. In 2D PhC structure, the periodicity of the dielectrics occurs in two directions. An example of the 2D PhC is the periodically arranged system of air holes in the silicon substrate or a lattice of dielectric rods in air. If three dimensions in the photonic crystal structure have permittivity modulation, the structure will be called 3D PhC. 1D, 2D, and 3D PhC structures are shown in **Figure 1**.

Photonic band gap (PBG) is the important property of the photonic crystals. PBG mentions to forbidden frequency or wavelength range in PhC structure. However, a little change in the periodic structure, which is called as defect, can create a new frequency range in the band gap [1]. In the lattice of air holes in silicon, defects can be formed by reducing or increasing the radius of one or more air holes; even defects can be shaped by filling holes.

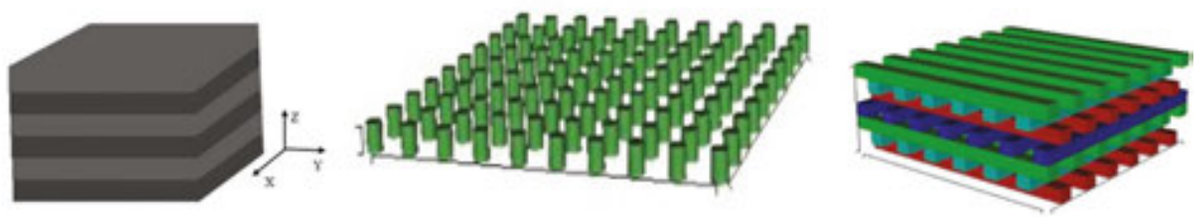

Figure 1. Photonic crystal structures (a) 1D, (b) 2D, and (c) 3D [1].

The photonic crystals have been presented by various structures and have been used in various applications. These structures such as fibers, waveguides, cavities, micro- and nano-resonators, and ring resonators and also their applications including photonic crystal multiplexers, photonic crystal filters, photonic crystal lasers, photonic crystal sensors, etc., have been reported.

Photonic crystals can be fabricated by complementary metal–oxide–semiconductor (CMOS) techniques and because of the unique capability to control light in small dimensions are excellent platforms for ultra-sensitive sensors to small changes in the refractive index. These advantages and other benefits caused photonic crystal sensors as a strong sensing platform [2]. Photonic crystal sensors have been designed to detect different parameters such as gas, pressure, displacement, chemical, and biochemical molecules [3–8].

In photonic crystal chemical and biochemical sensors, the analysis is mainly done by two methods: two-dimensional finite-difference time-domain (2D-FDTD) and plane-wave expan-

http://dx.doi.org/ 10.5772/63288

sion (PWE) approaches. The propagation of electromagnetism wave can be simulated by the 2D-FDTD method and the PBG can be calculated with the PWE approach.

In this section, an overview of the photonic crystal chemical and biochemical sensors is discussed.

2. Sensing mechanism in the photonic crystal chemical sensor

Two detection protocols can be used in optical chemical and biochemical sensors: fluorescent-based detection and label-free sensing [2]. In fluorescent-based detection, the biological molecules are altered. The biological molecules are labeled by fluorescence, and then, the intensity of the sensor output is measured. The measured intensity is used to represent the presence of biological molecules. But, in label-free sensing, the target biological molecules are not labeled and are detected in their natural forms.

The label-free based chemical/biochemical sensors were reported to variety of methods such as surface plasmon resonance, interferometer, waveguide, fiber, ring resonator, and photonic crystal [2]. Among these methods, the method based on the photonic crystals has been more attention.

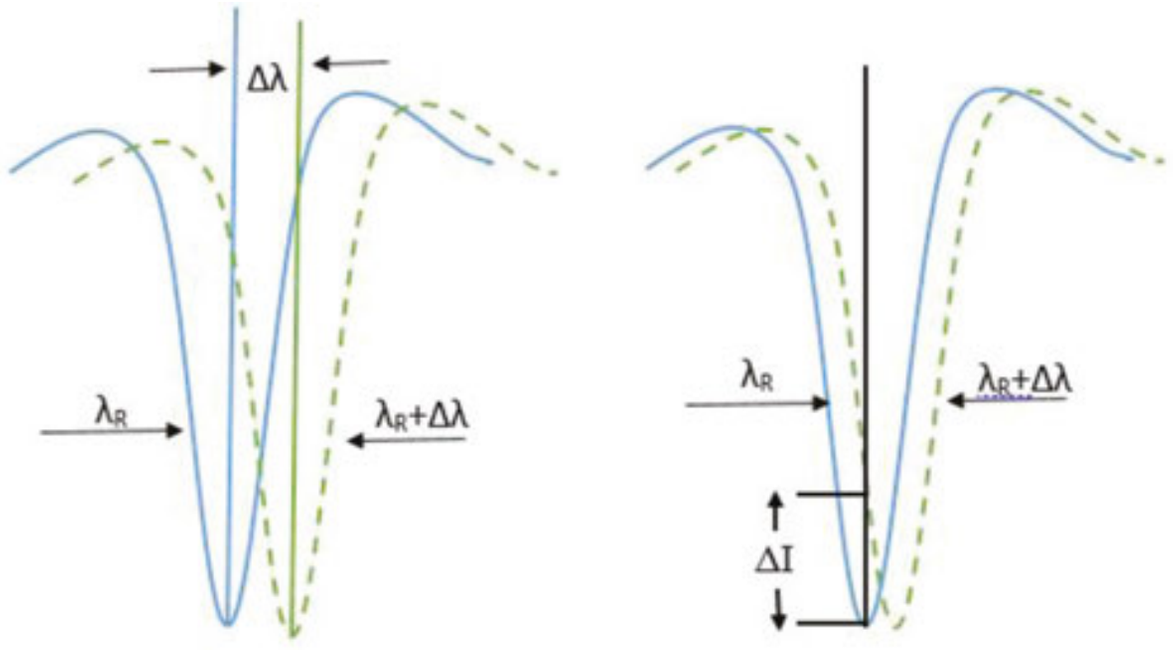

Figure 2. (a) Resonant wavelength shift pattern and (b) intensity variation pattern.

Sensing mechanism in the most photonic crystal sensors is similar in the use of refractive index (RI) change mechanism. The RI change does not depend on the total sample mass but depends on the surface density. When nano-measurement is involved, this characteristic will be very important.

In RI change mechanism, when the biological molecules inject to the optical sensor, the biological molecules bind to active sensing surface. As a result, the refractive index of the active sensing surface will be changed. So, some of the characteristics of the transmission spectrum will be changed. This process can be used as a way to measure the concentration of the biological molecules [9].

In the first category, to identify the presence of biological molecules, the amount of changes in the resonance wavelength is calculated (see **Figure 2(a)**). This method is based on the resonant wavelength shift (RWS) scheme. This scheme is used to measure a wider range that is determined by the free spectral range (FSR). To improve the accuracy of sensor based on RWS-scheme, achieving narrow full width at half maximum (FWHM) is very important. Using this method, the tiny shift in the effective refractive index cannot be measured. For this measurement, high sensitivity sensor is required.

In the second category, to identify the presence of biological molecules, the amount of the intensity change at the resonant frequency is measured. This method is based on the intensity variation (IV) scheme (see **Figure 2(b)**). In this case, a broader FWHM will be desirable and only a small range of wavelength shift can be calculated.

3. Important parameters in sensing applications

Compact optical devices with high quality can be made by precise control in geometric parameters, which some of them have inconsistency. Thus, in biosensing applications, they should be selected so that the optimum state is achieved. Some of the most important parameters of the sensor are as follows.

3.1. Quality factor

Quality factor is the ratio of resonant wavelength (λ_{res}) to the full width at half maximum (FWHM) of drop waveguide output ($\Delta\lambda$). Quality factor can be expressed as $\lambda_{res}/\Delta\lambda$ or $\omega/\Delta\omega_{FWHM}$, where ω is the resonant frequency and $\Delta\omega$ is the full width at half maximum.

3.2. Full width at half maximum (FWHM)

Full width at half maximum is an important parameter to design the sensor, because it affects the quality factor and detection limit (DL). As FWHM be more narrowed, the quality factor and detection limit will be better. With increment of loss, FWHM is increased.

3.3. Free spectral range (FSR)

Free spectral range should be sufficiently wide that adjacent resonant peaks do not interfere in operation of the working resonant peak. FSR is directly proportional to the square of the wavelength. Thus, in the shorter wavelengths, FSR will be smaller. Since the wavelength has a more impact on the FSR, design of sensor in longer wavelengths is the easiest way for optimization of the FSR. In sensors that the presence of the analyte is determined, FSR is not

very important parameter. Sensors that use the change density method for the sensing have small FSR. But the sensors that use resonant wavelength shift method with large scale need to wider FSR.

3.4. Detection limit (DL)

Detection limit is the minimal physical change that can be detected. It can be calculated by DL = FWHM/*S*, where *S* is the sensitivity. The detection limit in homogenous sensing can be defined as the smallest changes in the refractive index unit which sensor can detect. Detection limit is minimal increasing the thickness of add-layer that is formed by binding biomaterial to sensing surface.

3.5. Sensitivity

Sensitivity is the wavelength shift per weight of biomolecule in femto-gram unit or, according to another definition, wavelength shift per refractive index unit.

4. Photonic crystal chemical/biochemical sensors

Most of the photonic crystal biosensors are able to detect chemical and biochemical molecules. Biosensors can be designed according to different photonic crystal structures such as photonic crystal fibers [10, 11], photonic crystal-based waveguides [12, 13], photonic crystal-based resonators [14–20], and ring resonators [21–24]. Now, research on the photonic crystal resonator-based sensors has more attention. In the following, some of the biosensors or biochemical sensors have been presented.

4.1. Biosensor or biochemical sensors based on photonic crystal resonators

The biosensors or biochemical sensors usually have a resonator and one or two waveguides. The resonator plays the role of sensing hole. In the resonator, since light is strongly limited, quality factor is improved.

4.1.1. Photonic crystal biosensor with wide measurement range

Olyaee and Najafgholinezhad were introduced a biosensor based on nano-cavity for identification of chemicals and biomaterial molecules such as DNA and protein [14]. The basic structure of the biosensor is illustrated in **Figure 3(a)**. The structure consists of a nano-cavity and two end waveguides. The nano-cavity is obtained by reducing radius of one air hole in the middle of the photonic crystal structure and the two waveguides are formed by eliminating a row of air holes.

In the structure design, many parameters such as the size of nano-cavity hole, the coupling distance, and the length of the input and output waveguides have been calculated. To select the appropriate value for the size of the nano-cavity, the transmission spectra and the quality factor have been studied with for different sizes of defects. As shown in **Figure 3(b)** and **(c)**,

for different radii of the defect, the quality factor has a maximum value for the radius equal to 80 nm. In this study, in order to have the high output, $R_{in} = 0.6R$ and $R_{out} = 1.4R$ are considered, where R is the radius of the air holes.

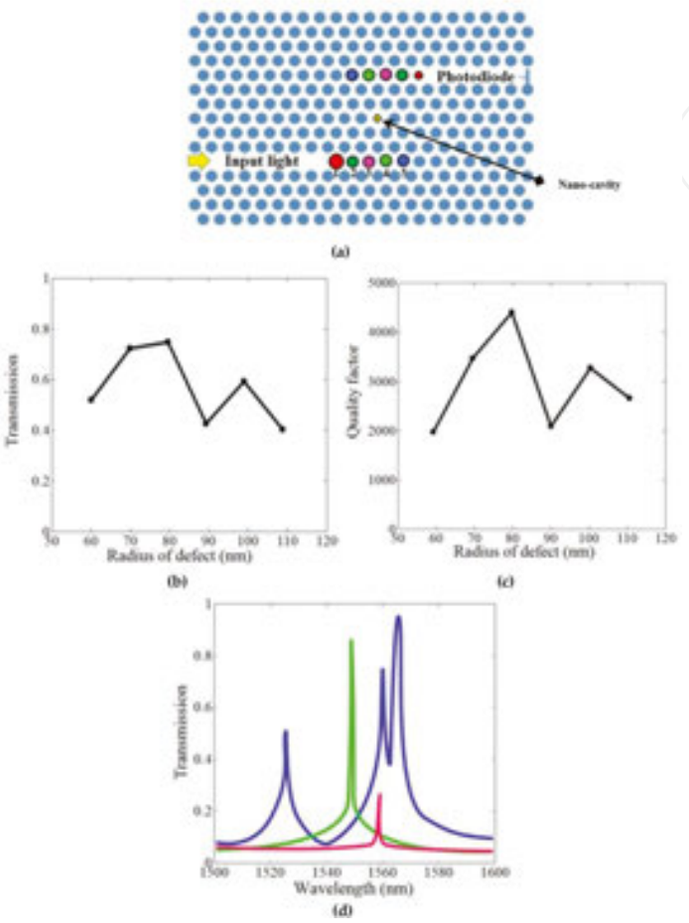

Figure 3. (a) The basic structure of the biosensor, (b) the transmission spectrum, (c) the quality factor for different sizes for nano-cavity, and (d) the transmission spectrum in three states for coupling distance [14].

Also, in this structure, the distance between the waveguides and nano-cavity has been investigated. In **Figure 3(d)**, the transmission spectrum in three states with one (blue curve), two (green curve), and three (red curve) rows of holes as coupling distance is depicted. In the case of one row for coupling distance, the disturb mode is appeared in transmission spectra. If the third row of holes is between the waveguides and the resonator, the intensity of spectrum transmission will be a sharp reduction. But with two rows of holes as distance coupling, the intensity transmission spectrum is desirable and the sensor presents the high quality factor. For a good coupling between the waveguide and nano-cavity, choosing the length of waveguides is important. The length is studied at five states. In each case, the transmission spectra are measured. The output transmission spectra at the five cases can be observed in **Figure 4(a)**. Choosing the three, four, and five states are not suitable and the quality factor of the state 1 is more comparing to the quality factor of state 2. So the state 1 is intended to select the

http://dx.doi.org/ 10.5772/63288

length of the waveguides. **Figure 4(b)** shows the transmission spectrum of the biosensor by changing the refractive index in the range of 1.00–3.00. The resonant wavelength is shifted to the longer wavelengths by increasing the refractive index. The parameters in sensing application include the quality factor, sensitivity, and regression coefficient that are, respectively, obtained as 5248, 55 nm/RIU, and 0.99923.

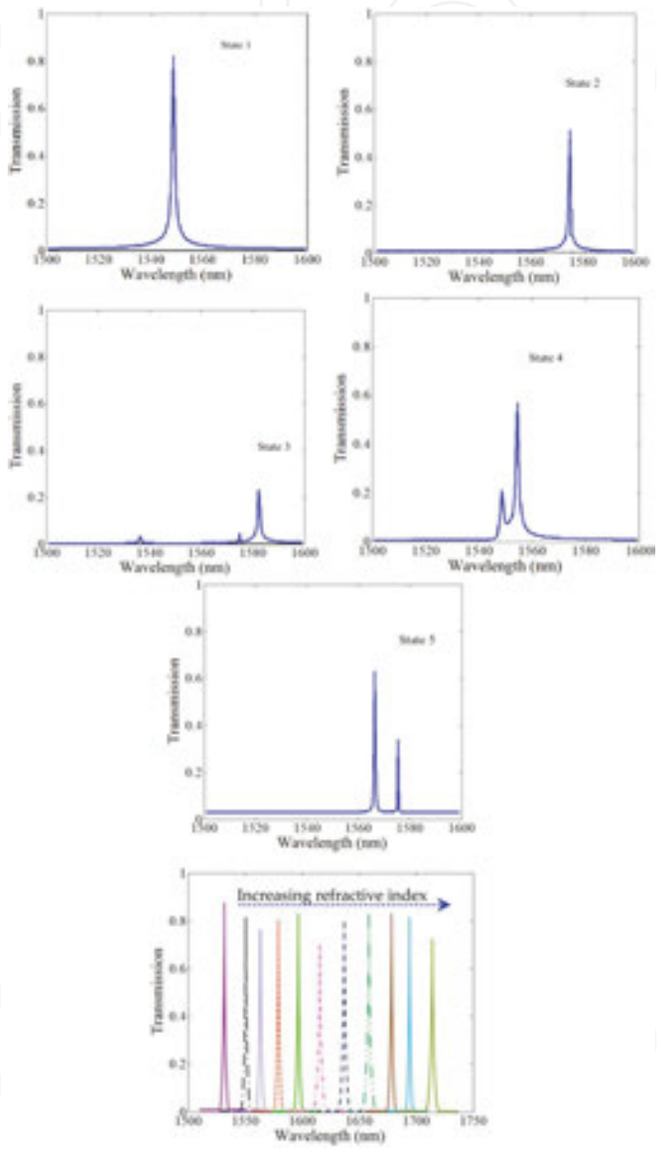

Figure 4. (a) The output transmission obtained by waveguides' length variation for five states and (b) the transmission spectrum of biosensor for some refractive indexes in the range of 1.00–3.00 [14].

4.1.2. Biosensor-based photonic crystal micro-resonator to detect small changes in the refractive index

In 2003, the biosensor based on the photonic crystal micro-resonator was introduced to detect small changes in the refractive index [15]. The sensor was suitable to detect many chemical or biochemical molecules. The transmission spectra of the sensor have a resonance wavelength

within the wavelength range of 1.5 μm and the quality factor was equal to 400. The structure was responsive to changes in the refractive index in the range of 1–1.5. The micro-resonator was formed by decreasing the size of the air hole in the center of the structure. The general layout of the structure is represented in **Figure 5(a)**. By changing the refractive index as 1.446, 1.448, 1.450, 1.452, and 1.454, the resonant peak is shifted to about 1500.2 nm, 1500.8 nm, 1501.2 nm, 1501.7 nm, and 1502.1 nm, respectively, as shown in **Figure 5(b)**.

4.1.3. Photonic crystal biosensor based on waveguide and nano-cavity

A new sensor for sensing DNA molecules has been investigated in 2016 by Mohsenirad et al. [16]. The structure of this biosensor consists of hexagonal lattice of air holes in a silicon slab and its operation based on two waveguides and nano-cavity that have been created in this lattice. Pulse is applied to waveguide 1, then resonant mode of resonator is excited, and output signal is recorded at the end of waveguide 2. In recorded transmission spectra, the result of interaction between trapped light and analyte into sensing hole is appeared in the form of resonant peak shift. As shown in **Figure 6(a)**, nano-resonator has been created by reducing the radius of an air hole.

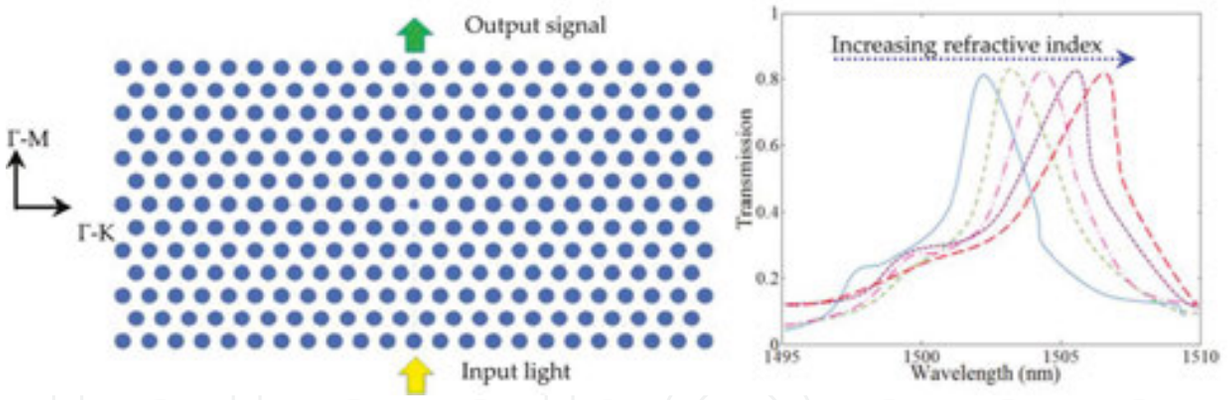

Figure 5. (a) The layout of photonic crystal structure of the biosensor based on micro-resonator to detect small changes in the refractive index and (b) the transmission spectrum of structure for binding biochemical with different refractive indexes [15].

In this structure, physical parameters such as position of resonator, length of the waveguides, radii of the defect, and coupling distance have been investigated in order to achieve an optimized sensor for biochemical sensing applications. In order to choice the best size for nano-resonator, the radius of defect has been studied in the range of 80–100 nm that according to **Figure 6(b)**, the radius of 95 nm has been selected. By increasing the size of sensing hole, sensitivity increases; thus, larger radius is desirable. But quality factor as another important parameter for biosensing applications is contrast with sensitivity.

http://dx.doi.org/ 10.5772/63288

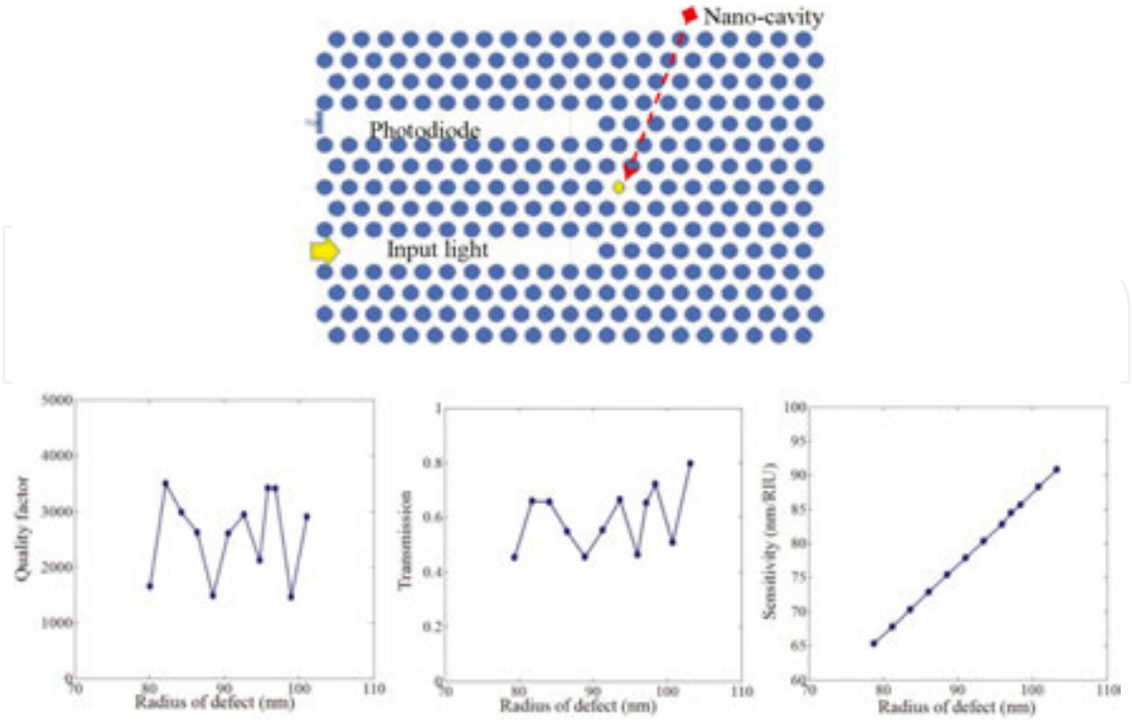

Figure 6. (a) The schematic of photonic crystal biosensor and (b) the sensing parameters of PhC sensor [16].

Since the cavity position affects the sensing parameters of biosensor, transmission spectra of structure for different positions (holes H_1, H_2, and H_3) as are shown in **Figure 7(a)** have been investigated that according to simulation results, H_3 has been selected as the best position.

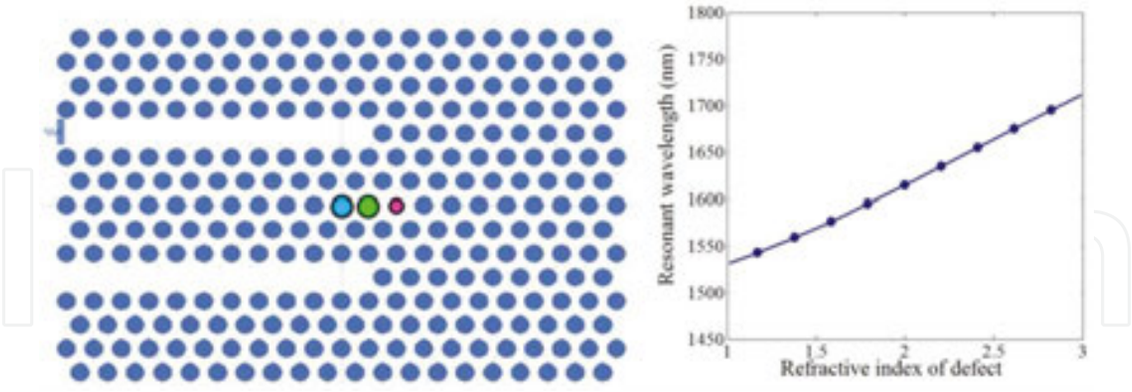

Figure 7. (a) The position of the sensing hole for the nano-resonator (H_1, H_2, and H_3 are, respectively, marked by blue, green, and red holes) and (b) the quasi-linear relation between resonant wavelength and refractive index of defect [16].

Another parameter that in this design has been studied is the length of the waveguide. According to the investigations, when waveguides have been created by eliminating more than 11 holes, spurious modes appeared. The best result for waveguide length is 11 holes. In this design, two rows of air holes have been selected as coupling distance, because by selecting one period as coupling distance, quality factor decreases and spurious mode appears. Also in

increment of coupling distance of three periods, light coupling gets difficult and sensitivity decreases.

This biosensor is able to measure a wide range of refractive index of 1.00–3.00 with sensitivity of 83.75 nm/RIU and quality factor of 3051. Also this sensor has quasi-linear operation with correlation coefficient of 0.99954 that is shown in **Figure 7(b)**.

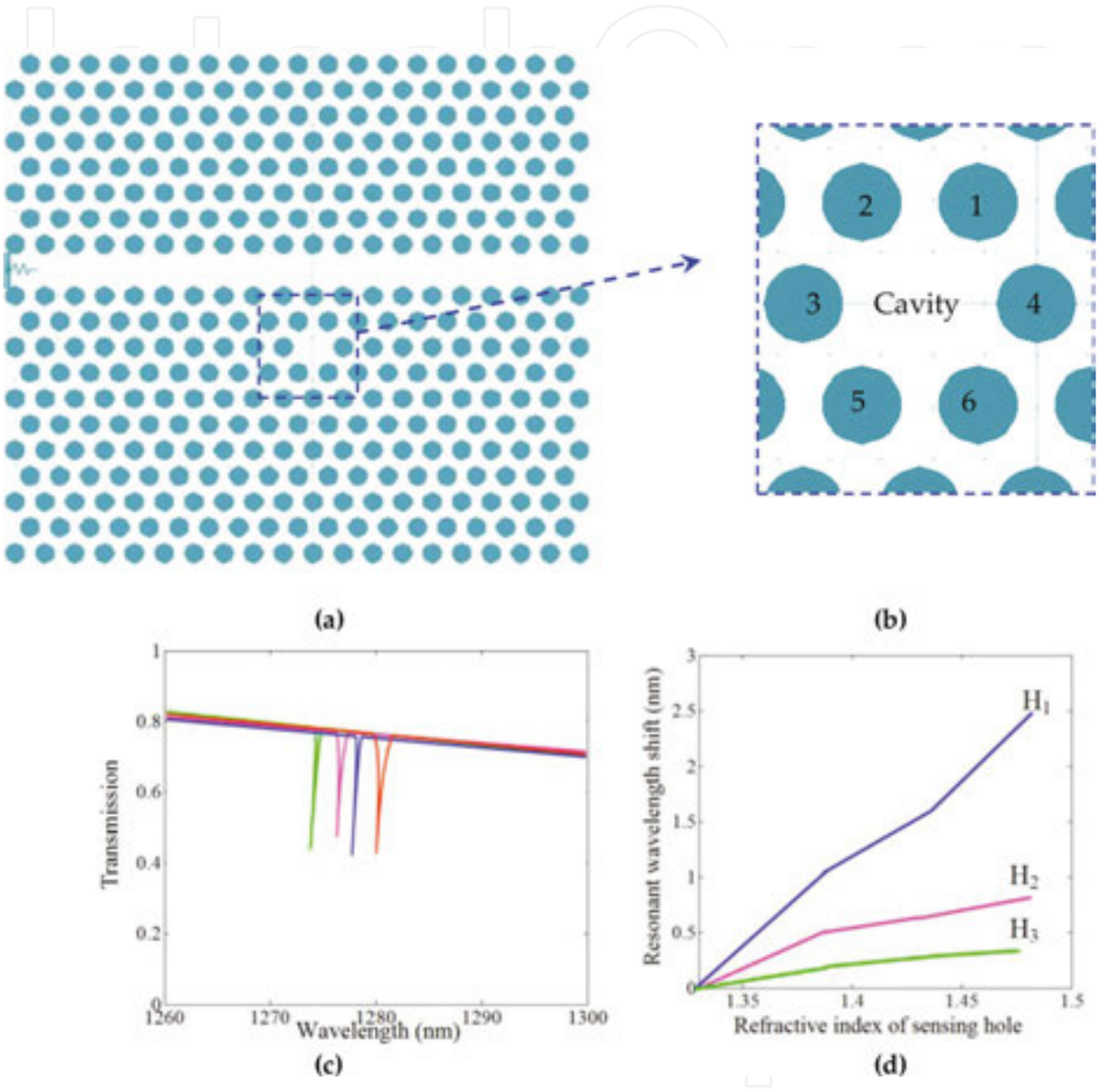

Figure 8. (a) Photonic crystal biosensor based on nano-cavity, (b) layout of nano-cavity and six labeled holes, (c) longer wavelength shift for H_1 compared to the wavelength shift for H_2 and H_3 in transmission spectra of biosensor (H_1, H_2, H_3, and reference are shown as orange, red, blue, and green curves) and (d) the higher sensitivity for H_1 [17].

4.1.4. Biosensor based on nano-resonator

In the biosensor based on nano-resonator structure, the resonator has been created by omitting an air hole and selecting an air hole adjacent to it as the best sensing hole [17]. In this sensor, a waveguide has been considered for applying optical pulse and recording output signal. In

http://dx.doi.org/ 10.5772/63288

Figure 8(a), nano-cavity and waveguide or in other words point and line defects are shown. Sensing mechanism is based on resonant wavelength shift that this shift caused by the binding biochemical to bioreceptor.

The best position of the sensing hole and coupling distance for obtaining optimized sensor parameters with high quality factor and sensitivity are investigated. For this purpose, six holes around the cavity labeled H_1, H_2, H_3, H_4, H_5, and H_6 are considered as shown in **Figure 8(b)**. Any of these holes was considered as a sensing hole and their effective refractive index variation due to injecting biochemical was investigated.

In **Table 1**, quality factor values and wavelength shift for any hole as a sensing hole are listed. According to **Table 1**, H_1, H_2, and H_3 are roughly equal to H_6, H_5, and H_4, respectively, because of symmetry. By choosing H_1 as sensing hole, resonant wavelength shifts more than other cases, as shown in **Figure 8(c)**. Thus, higher sensitivity is obtained by H_1 as a sensing hole, as shown in **Figure 8(d)**. Among all holes, H_1 has been selected for sensing hole because of its high quality factor and wavelength shift.

Sensing hole	Wavelength shift (nm)	Quality factor
H_1	2.2	4267.67
H_2	0.4	4261.67
H_3	0.9	2558.00
H_4	0.9	2558.00
H_5	0.4	4261.67
H_6	2.2	3200.75

Table 1. List of resonance wavelength shift and quality factor for different sensing holes [17].

Also, the effect of coupling distance has been studied and two rows of air holes were selected as coupling distance between resonator and waveguide. Investigations indicated that with increment of distance, quality factor is increased but sensitivity and output intensity are decreased.

Sensitivity of this sensor is calculated as 165.45 nm/RIU for the refractive indices of 1.00–1.33. Quality factor and detection limit of sensor are ~4000 and 1.2×10^{-3} RIU, respectively.

4.1.5. Multichannel photonic crystal biosensor

Multichannel photonic crystal biosensor consists of some cavities and a waveguide that any cavity has separate operation. This sensor with three cavities is shown in **Figure 9(a)** [17]. The biosensor is able to sense three specific refractive indices simultaneously. In this design, in

order to obtain resonators with different resonant wavelengths, the sensing holes have been shifted. By displacing marked hole in **Figure 9(a)**, resonant wavelength shifts, and therefore, new resonant wavelength is appeared as shown in **Figure 9(b)**.

Channels 2 and 3 have been created by deleting an air hole and displacing the sensing hole equal to 0.2 μm and 0.3 μm, respectively. Channel 1 has been obtained by deleting a hole without any displacement. The resonant wavelengths of channels 1, 2, and 3 are 1281.1 nm, 1286.6 nm, and 1296.1 nm, respectively, as shown in **Figure 9(c)**.

Figure 9(d) illustrates the separated operation of channels of multichannel biosensor. In **Figure 9(d)**, refractive index of channel 3 has been changed from 1.00 to 1.45, while refractive index of two other channels has not been changed. The resonant wavelength of channel 3 has been shifted to longer wavelengths, but resonant wavelength of channels 2 and 3 has remained stable. Sensitivity and detection limit of channel 3 have been calculated as S = 1.185 nm/RIU and 0.084 fg, respectively (assuming the injection DNA molecules to sensing hole).

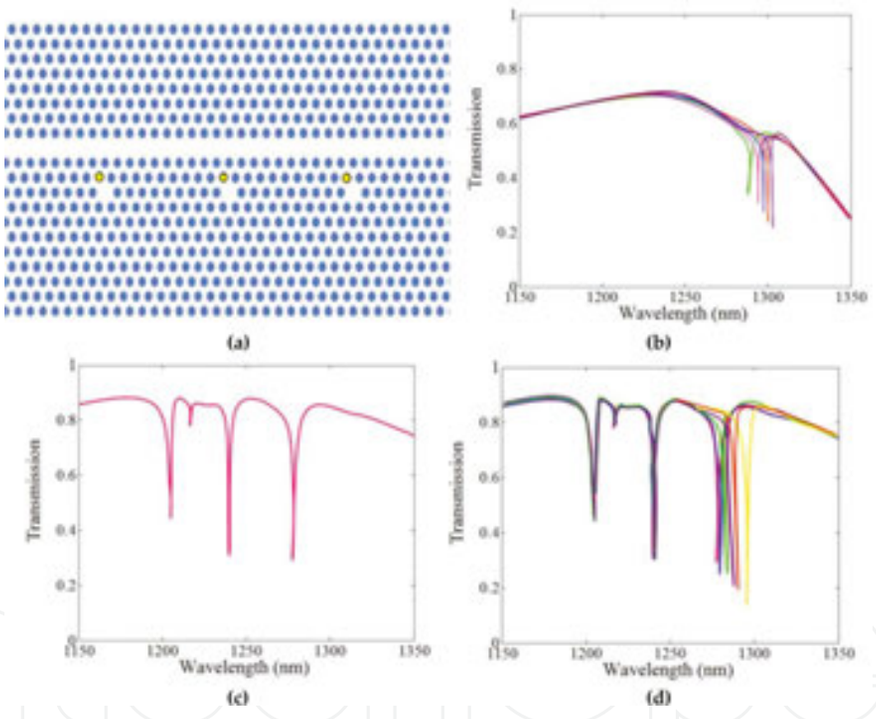

Figure 9. (a) The structure of multichannel biosensor, (b) the effect of sensing hole on transmission spectra, (c) the transmission spectra of multichannel biosensor without any analyte, and (d) transmission spectra of multichannel biosensor for injecting DNA molecules to channel 3 [17].

4.2. Biosensor or biochemical sensor based on photonic crystal LX resonator

In the biosensors and biochemical sensors, another resonator that has been introduced and used is LX resonators. This resonator is formed by removal of the successive air holes of structure which X represents the number of removed holes. In other words, X is the resonator length. For example, L3 resonator is obtained by removing three air holes in the photonic

crystal structure. Some of the resonators, namely, L3, L4, L7, and L13, have been provided [18–22]. Some of these sensors based on LX resonators are given in **Figure 10**.

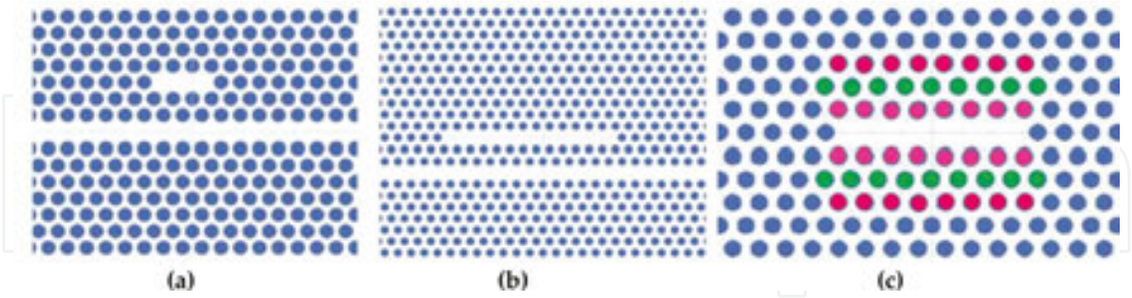

Figure 10. Photonic crystal LX resonators that are suitable for biosensor: (a) L3, (b) L13, and (c) L7 resonators [18–22].

The photonic crystal biochemical sensor based on L4 resonator has been developed in 2005. It was a biochemical sensor for detection of cations and anions [19]. The resonance wavelength of sensor was around 1.5 and the quality factor was obtained about 300–800.

According to conducted research on L3 resonator, Liu and Salemink were reported L7-resonator structure for biosensor applications [20]. The basic parameters of photonic crystal structure such as the lattice constant, the radius of the hole, and the thickness of the silicon slab were selected in such a way that the wavelength was near 1550 nm. The L7 resonator by setting several small holes has been amended. The quality factor of the sensor was 2600. Comparison of simulation results of binding ethanol and water showed that a change in the refractive index equal to 0.03 leads to a change of 12.5 nm in resonance wavelength of transmission. Therefore, a high sensitivity sensor can be created.

Photonic crystal biosensor based on L13 resonator had a high quality factor equal to 9300 [21, 22]. This biosensor has been used to detect protein.

4.3. Biosensor or biochemical sensor based on photonic crystal ring resonator

One of the photonic crystal structures that are used for biosensor applications is the ring resonator [8, 23–26]. For increasing the quality factor and sensitivity of the sensor, reduction of the radius of the ring can be very important. The sensing mechanism of this biosensor or biochemical sensor is based on the measurement of the refractive index change. In continuation, some examples of the biosensor or biochemical sensor based on photonic crystal ring resonator have been presented.

4.3.1. Biosensor based on photonic crystal diamond-shaped nano-ring resonator

Recently, a diamond-shaped nano-ring resonator for biochemical sensing applications has been investigated [23]. Sensing mechanism of sensor is based on RI change mechanism of label-free detection. By binding biochemical molecules to sensing hole, the refractive index will be changed. Thus, the resonance wavelength of the transmission spectrum shifts to longer wavelengths. Defects into the photonic crystal structure are formed by reduction of radius of

air holes and are included of a diamond-shaped ring resonator and two end waveguides. The size of ring diameter is equal to three rows of holes. Sketch of the biosensor is shown in **Figure 11(a)**.

In design of the structure, several parameters including reduction of defect holes radius, the end point of the waveguides, and the best holes for attaching chemical or biochemical molecules have been studied [24]. Selecting the best size for the air holes in defect, the R_w/R_a (ratio of the size of the holes of the defect to the size of the air holes) in the range of 0.26–0.39, has been altered. In any case, the quality factor and the intensity of transmission spectra have been measured. According to the results shown in **Figure 11(b)** and **(c)**, the size of 40.8 nm is selected.

For the best point to finish waveguides, five cases have been investigated. The five point cases are marked in **Figure 11(a)**. By comparing all simulation results, the end points, namely, "in ew 4" and "out ew 4," are the best holes to end the waveguide (see **Figure 11(d)**).

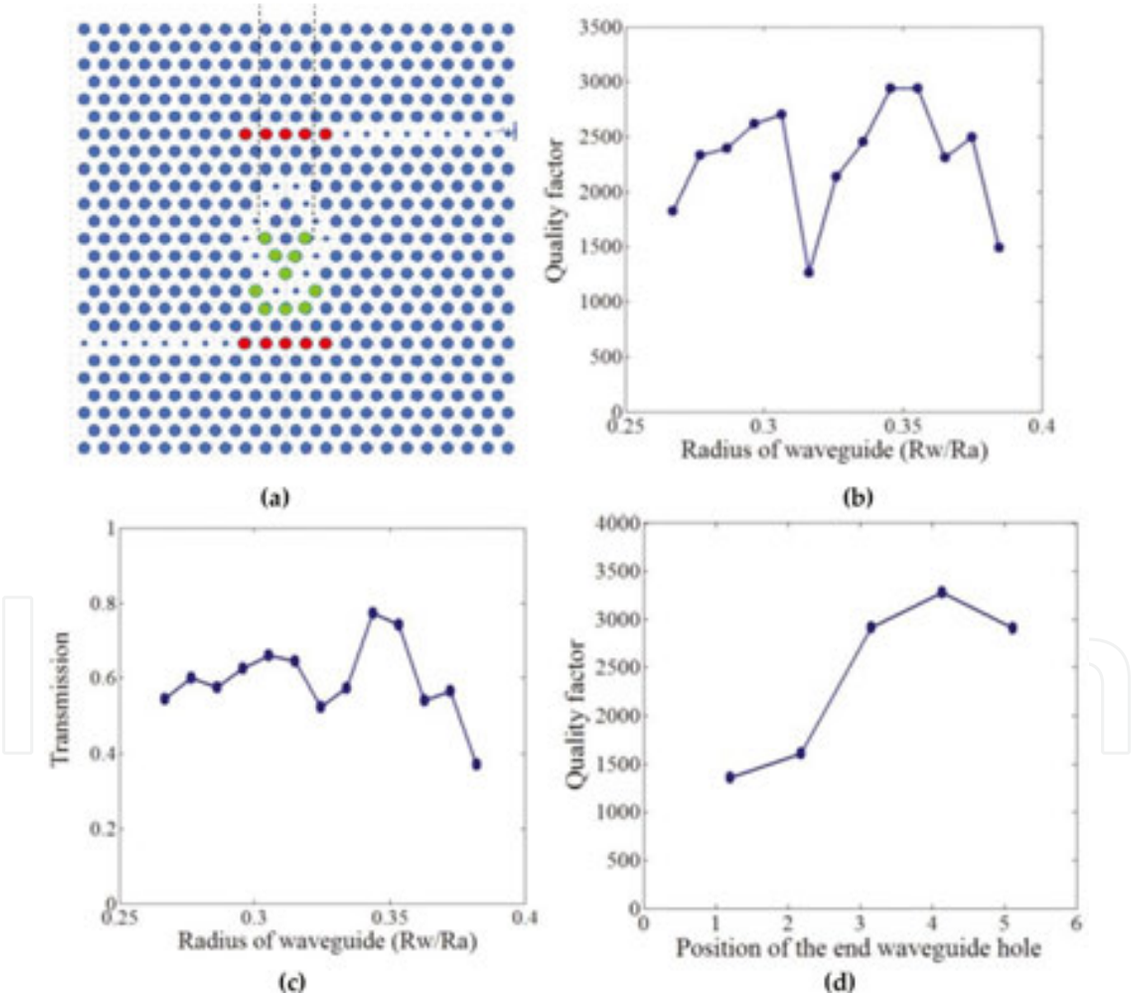

Figure 11. (a) Sketch of the biosensor based on photonic crystal diamond-shaped ring resonator for biochemical sensing applications where the red and green holes indicate position of ew and SHx holes, respectively, (b) the quality factor with respect to the radius of waveguide, (c) the intensity of transmission spectrum, and (d) the quality factor for various end-point waveguides [24].

http://dx.doi.org/ 10.5772/63288

Also, 10 air holes around the ring resonator for binding biochemical molecules have been studied. The 10 holes, namely, SHx, are shown in **Figure 11(a)**. After attaching the DNA molecule into each holes, the resonance wavelength shift and quality factor are measured. The results have been presented in **Table 2**. Based on the results, the SH_1 can be selected as the sensing hole.

	Sensing hole	Resonant wavelength (nm)	Resonant wavelength shift (nm)	Quality factor
$n = 1$	REF (Reference)	1468.0	–	3716
$n = 1.45$	SH_1	1473.1	5.1	3683
	SH_2	1468.6	0.6	1538
	SH_3	1468.6	0.6	3497
	SH_4	1468.6	0.6	3338
	SH_5	1468.6	0.6	3671
	SH_6	1469.9	1.9	3266
	SH_7	1469.5	1.5	1427
	SH_8	1469.9	1.9	3674
	SH_9	1469.3	1.3	3498
	SH_{10}	1469.9	1.9	3674

Table 2. List of resonance wavelength shift and quality factor for different sensing holes [24].

A relatively large range of refractive index in the sensor from 1.33 to 1.54 is detected. The quality factor of the sensor is about 3700 and the sensitivity of biosensor for DNA detection is 3.4 nm/fg.

4.3.2. Two-curve-shaped (TCS) biosensor for detecting small refractive index variations

In some identification of chemical or biochemical molecules, a sensor is required to detect small refractive index changes. A novel design of TCS biosensor has been reported in [25]. The biosensor is constructed based on photonic crystal using the hexagonal lattice of air holes in dielectric slap (see **Figure 12(a)**). Defects into the structure consist of a ring resonator and two waveguides. The defects are configured by removing one or several of air holes. The coupling distance is equal to two rows of air holes. Sensing mechanism of TCS biosensor is based on the IV scheme. By filling sensing hole with chemical or biochemical molecules, the intensity of the transmission spectrum is shifted to lower values.

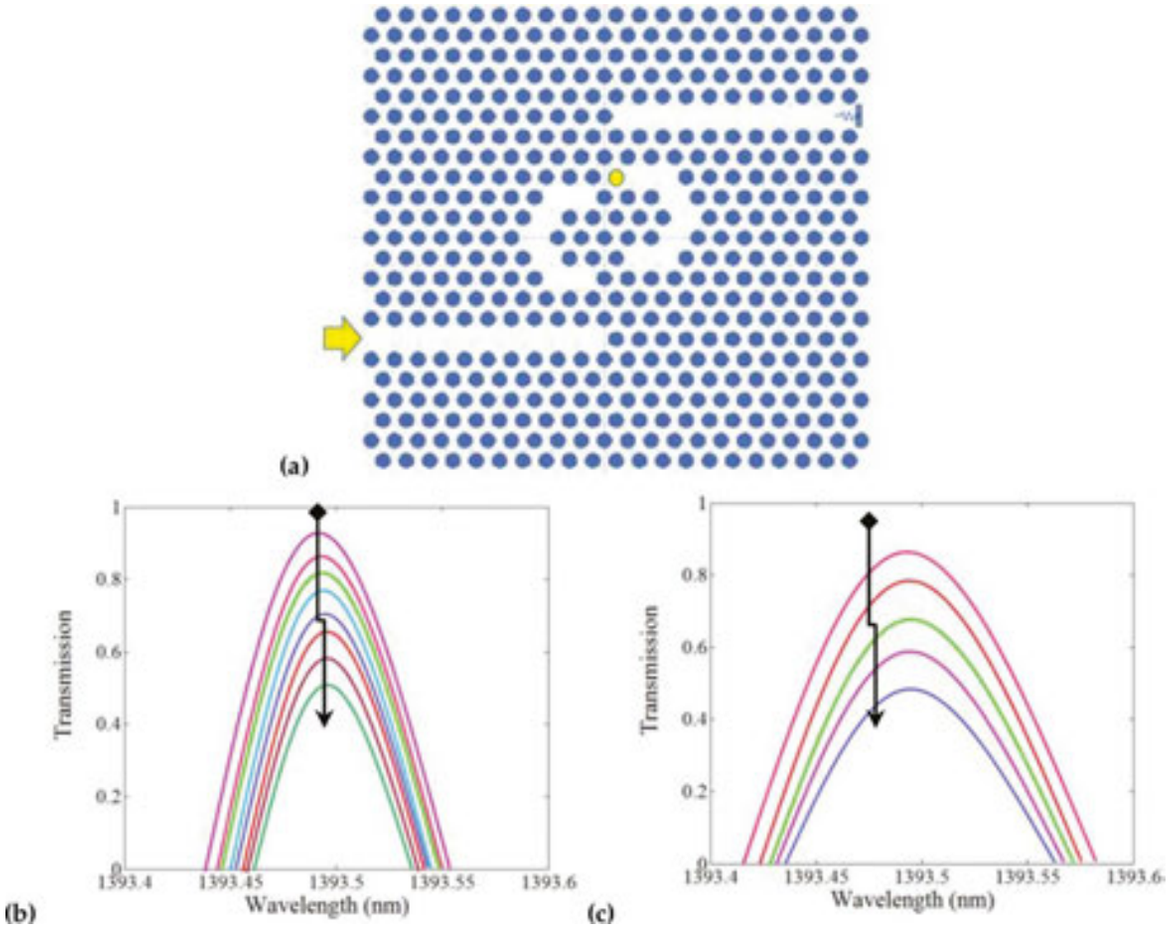

Figure 12. (a) TCS biosensor based on photonic crystal nano-ring resonator (the sensing hole is marked on the structure as yellow hole) [25] and the resonant wavelength of the TCS biosensor when the sensing hole is filled by various biochemical molecules, (b) salt levels of sea water, and (c) glucose concentration (increasing salt level and glucose concentration are shown by arrows) [8].

The present sensor can be used for the detection of the sea water salinity and identification of the glucose concentration [8]. The transmission spectrum when sensing hole plugging by sea water with different salinities is presented in **Figure 12(b)**. Also, the transmission spectrum is shown in **Figure 12(c)** for different percentages of glucose solution attached to the sensing hole. According to **Figures 12(b)** and **12(c)**, in the both cases, the intensity is reduced by increasing concentration.

4.3.3. A novel photonic crystal nano-ring resonator for biochemical sensor applications

Another structure of biochemical sensor is presented that is based on nano-ring resonator shaped by two consecutive curves. One of the curves is made by removing seven air holes [26]. A waveguide to apply light is located at the bottom of the structure. The light from top waveguide is detected by a photodetector. The layout of the biochemical sensor is demonstrated in **Figure 13**. According to **Figure 13**, the coupling distance is considered equal to two rows.

The number of rows between the two curves is expressed in horizontal distance. To have a suitable horizontal distance, this is studied in four states. In the each case, the quality factor and intensity of spectrum transmission are calculated, as shown in **Figure 13(b)** and **(c)**.

The vertical distance meant that curve 2 is several rows higher than curve 1. To examine the vertical distance, the distance from zero to six rows of holes is selected. **Figure 13(d)** and **(e)** presents the results of these modes including the quality factor and the intensity of spectrum transmission.

To check the suitability of the structure for sensing, the refractive index of sensing hole is changed in the range of 1.33–1.48. The normalized curve is shown in **Figure 13(f)**. This curve demonstrates a relatively linear relationship between changes in the refractive index and the intensity shift of transmission spectra. Regression coefficient of the biosensor is obtained about 0.99967. By a unit change in the refractive index of the biochemical sensor, the intensity of transmission spectrum is reduced to 14.26 units.

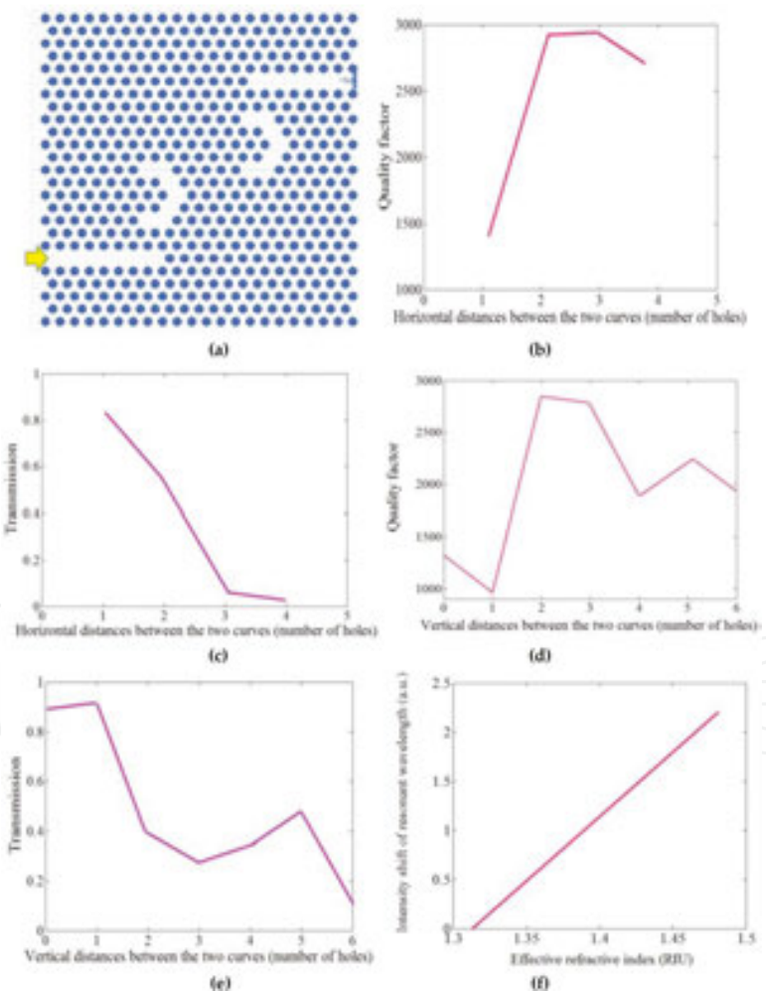

Figure 13. (a) The preliminary layout of the biochemical sensor, (b) the quality factors and (f) the intensity of the resonance wavelength in various horizontal distances between the two curves, (c) the quality factors and (d) the intensity of the resonance wavelength in various vertical distances between the two curves, and (e) the intensity shift of resonant wavelength with respect to the effective refractive index [26].

5. Conclusion

In this chapter, photonic crystals and detection methods in chemical sensors have been described. Also, the most important parameters in sensing applications, such as quality factor, detection limit, and sensitivity, have been introduced. In addition, several sensors based on photonic crystal structures for using chemical or biochemical sensing were investigated. The photonic crystal structures used in presented sensors included resonators or nano-ring resonators. Most of them were based on resonant wavelength shift and the rest were based on the intensity variation scheme. Due to the positive indicators for photonic crystal sensors, they can be appropriate structures for nanotechnology research, food processing, pharmaceutical industry, biology, and environmental applications.

Author details

Saeed Olyaee*, Hamideh Mohsenirad and Ahmad Mohebzadeh-Bahabady

*Address all correspondence to: s_olyaee@srttu.edu

Nano-photonics and Optoelectronics Research Laboratory (NORLab.), Faculty of Electrical Engineering, Shahid Rajaee Teacher Training University (SRTTU), Lavizan, Tehran, Iran

References

[1] J. D. Joannopoulos, S. G. Johnson, J. N. Winn, R. D. Meade, "Photonic crystals molding the flow of light", Princeton University Press, 2007, ISBN: 978-0-691-12456-8.

[2] X. Fan, I. M. White, S. I. Shopova, H. Zhu, J. D. Suter, Y. Sun, "Sensitive optical biosensors for unlabeled targets: A review", Analytica Chimica Acta 620, pp. 8–26, 2008.

[3] S. Olyaee, A. Naraghi, "Design and optimization of index-guiding photonic crystal fiber gas sensor", Photonic Sensors 3, pp. 131–136, 2013.

[4] S. Olyaee, A. Naraghi, V. Ahmadi, "High sensitivity evanescent-field gas sensor based on modified photonic crystal fiber for gas condensate and air pollution monitoring", Optik 125, pp. 596–600, 2014.

[5] S. Olyaee, A. A. Dehghani, "High resolution and wide dynamic range pressure sensor based on two-dimensional photonic crystal", Photonic Sensors 2, pp. 92–96, 2012.

[6] S. Olyaee, A. A. Dehghani, "Ultrasensitive pressure sensor based on point defect resonant cavity in photonic crystal", Sensor Letters 11(10), pp. 1854–1859, 2013.

[7] S. Olyaee, M. Azizi, "Micro-displacement sensor based on high sensitivity photonic crystal", Photonic Sensors 4(3), pp. 220–224, 2014.

[8] S. Olyaee, A. Mohebzadeh-Bahabady, "Two-curve-shaped biosensor for detecting glucose concentration and salinity of seawater based on photonic crystal nano-ring resonator", Sensor Letters 13, pp. 1–4, 2015.

[9] C. Y. Chao, L. J. Guo, Design and optimization of microring resonators in biochemical sensing applications, Journal of Lightwave Technology 24, pp. 1395–1402, 2006.

[10] M. T. Myaing, J. Y. Ye, T. B. Norris, "Enhanced two-photon biosensing with double-clad photonic crystal fibers", Optics Letters 28(14), pp. 1224–1226, 2003.

[11] E. Coscelli, M. Sozzi, F. Poli, D. Passaro, A. Cucinotta, S. Selleri, R. Corradini, R. Marchelli, "Toward a highly specific DNA biosensor: PNA-modified suspended-core photonic crystal fibers", IEEE Journal of Selected Topics in Quantum Electronics 16(4), pp. 967–972, 2010.

[12] S. C. Buswell, V. A. Wright, J. M. Buriak, V. Van, S. Evoy, "Specific detection of proteins using photonic crystal waveguides", Optics Express 16(20), pp. 15949–15957, 2008.

[13] M. G. Scullion, A. Di Falco, T. F. Krauss, "Slotted photonic crystal cavities with integrated microfluidics for biosensing applications", Biosensors and Bioelectronics 27, pp. 101– 105, 2011.

[14] S. Olyaee, S. Najafgholinezhad, "A high quality factor and wide measurement range biosensor based on photonic crystal nanocavity resonator", Sensor Letters 11, pp. 483–488, 2013.

[15] E. Chow, A. Grot, L. W. Mirkarimi, M. Sigalas, G. Girolami, "Ultracompact biochemical sensor built with two-dimensional photonic crystal microcavity", Optics Letters 29(10), pp. 1093–1095, 2004.

[16] H. Mohsenirad, S. Olyaee, M. Seifouri, "Design of a new two-dimensional optical biosensor using photonic crystal waveguides and a nanocavity", Photonics & Lasers in Medicine 5(1), 2016.

[17] S. Olyaee, S. Najafgholinezhad, "Computational study of a label-free biosensor based on a photonic crystal nanocavity resonator", Applied Optics 52(29), pp. 7206–7213, 2013.

[18] D. Dorfner, T. Zabel, T. Hürlimann, N. Hauke, L. Frandsen, U. Rant, G. Abstreiter, J. Finley, "Photonic crystal nanostructures for optical biosensing applications", Biosensors and Bioelectronics 24, pp. 3688–3692, 2009.

[19] S. Chakravarty, J. Topolanik, P. Bhattacharya, S. Chakrabarti, Y. Kang, M. E. Meyerhoff, "Ion detection with photonic crystal microcavities", Optics Letters 30(19), pp. 2578–2580, 2005.

[20] Y. Liu, H. W. M. Salemink, "Photonic crystal-based all-optical on-chip sensor", Optics Express 20(18), pp. 19912–19920, 2012.

[21] S. Chakravarty, W. C. Lai, Y. Zou, H. A. Drabkin, R. M. Gemmill, G. Simon, S. Chin, R. Chen, "Multiplexed specific label-free detection of NCI-H358 lung cancer cell line lysates with silicon based photonic crystal microcavity biosensors", Biosensors and Bioelectronics 43, pp. 50–55, 2013.

[22] S. Chakravarty, Y. Zou, W. C. Lai, R. Chen, "Slow light engineering for high Q high sensitivity photonic crystal micro cavity bio-sensors in silicon", Biosensors and Bioelectronics 38, pp. 170–176, 2012.

[23] S. Olyaee, A. Mohebzadeh-Bahabady, "A diamond-shaped bio-sensor based on two-dimensional photonic crystal nano-ring resonator", IEEE, IET 10th International Symposium on Communication Systems, Networks and Digital Signal Processing (CSNDSP 2014), 23–25 July 2014.

[24] S. Olyaee, A. Mohebzadeh-Bahabady, "Design and optimization of diamond-shaped biosensor using photonic crystal nano-ring resonator", Optik 126, pp. 2560–2564, 2015.

[25] S. Olyaee, A. Mohebzadeh-Bahabady, "Two-curve-shaped biosensor using photonic crystal nano-ring resonators", Journal of Nanostructures 4, pp. 303–308, 2014.

[26] S. Olyaee, A. Mohebzadeh-Bahabady, "Designing a novel photonic crystal nano-ring resonator for biosensor application", Optical and Quantum Electronics 47(7), pp. 1881–1888, 2015.